J Mater Sci: Mater Med (2010) 21:2255–2261
DOI 10.1007/s10856-009-3961-4

Hydroxyapatite bone substitutes developed via replication of natural marine sponges

Eoin Cunningham · Nicholas Dunne · Gavin Walker · Christine Maggs · Ruth Wilcox · Fraser Buchanan

Received: 18 September 2009 / Accepted: 30 November 2009 / Published online: 12 December 2009

Abstract The application of synthetic cancellous bone has been shown to be highly successful when its architecture mimics that of the naturally interconnected trabeculae bone it aims to replace. The following investigation demonstrates the potential use of marine sponges as precursors in the production of ceramic based tissue engineered bone scaffolds. Three species of natural sponge, Dalmata Fina (*Spongia officinalis Linnaeus,* Adriatic Sea), Fina Silk (*Spongia zimocca,* Mediterranean) and Elephant Ear (*Spongia agaricina*, Caribbean) were selected for replication. A high solid content (80 %wt), low viscosity (126 mPas) hydroxyapatite slurry was developed, infiltrated into each sponge species and subsequently sintered, producing a scaffold structure that replicated pore architecture and interconnectivity of the precursor sponge. The most promising of the ceramic tissue engineered bone scaffolds developed, *Spongia agaricina* replicas, demonstrated an overall porosity of 56–61% with 83% of the pores ranging between 100 and 500 μm (average pore size 349 μm) and an interconnectivity of 99.92%.

E. Cunningham (✉) · N. Dunne · F. Buchanan
School of Mechanical and Aerospace Engineering, Queen's University Belfast, Ashby Institute, Ashby Building, Stranmillis Road, BT9 5AH Belfast, UK
e-mail: ecunningham07@qub.ac.uk

G. Walker
School of Chemistry and Chemical Engineering, Queen's University Belfast, David Keir Institute, Belfast, UK

C. Maggs
School of Biology, Queen's University Belfast, Ashby Institute, Belfast, UK

R. Wilcox
School of Mechanical Engineering, University of Leeds, Leeds, UK

1 Introduction

An optimal scaffold for bone tissue replacement should fulfil several criteria; coupled with the use of a material known to induce the attachment and proliferation of cellular material necessary for integration key architectural parameters such as appropriate pore size distribution, interconnectivity of pores and surface porosity should also be achieved [1, 2]. Obtaining the optimum pore size distribution and interconnectivity, however, should not be achieved at the expense of structural integrity. At the very least a scaffold should have sufficient stability to maintain its architecture during in vitro culturing and handling throughout implantation. Once integration has occurred the implanted scaffold should function in tandem with neighbouring healthy bone and assume a shared load, reducing the risk of rejection and failure. If successful the stability of the implant should increase as reported by Sopyan et al. who found the compressive strength of porous HA implanted rose from 2 to 20 MPa 3 months after implantation [3].

As to the optimum pore size distribution, debate continues. Karageorgiou et al. [2], cite the development of several HA scaffolds, with pore sizes ranging from 150 to 800 μm, all of which have heralded some level of bone ingrowth. While Von Doernberg et al. [4] concur with this range, a number of authors including Sopyan et al., Giannoudis et al., and Eggli et al. [3, 5, 6], cite narrower ranges of 100–400, 150–500, and 250–300 μm, respectively. As far as pinpointing an optimum pore size within the ranges cited, the literature provides no clear conclusion. Von Doernberg et al. [4] discuss several contradictory investigations where increasing the pore size (within the 150–800 μm range) has seen; (I) increased bone ingrowth (II) decreased bone ingrowth and (III) no effect. The fact that these investigations do not yield

an optimum may elevate the importance of other requirements.

Of equal importance is the arrangement of pores, with interconnectivity cited as major contributory factor in the successful integration of a bone substitute scaffold with the host tissue. According to Klawitter and Hulbert [7] a minimum interconnection pore size of 40–100 and 5–15 μm will allow ingrown blood vessels to anastomose (diverge and reconnect) freely with each other facilitating mineralised bone and fibrous tissue ingrowth, respectively. In fact Bohner et al. [8] downplay the importance of pore size distribution; stating that bone ingrowth should not be affected by pore size as long as they are fully interconnected through openings larger than 50 μm. It is this interconnectvity between pores which promotes body fluid circulation and cell migration to the core of the implant [9, 10]. According to Mastrogiacomo et al. [11] incomplete interconnectivity can represent a constraint of the overall biological system, limiting blood vessel invasion (angiogenesis).

The presence of microporosity (pores $\leq$20 μm) is also important according to Hing et al. [12], providing increased surface area for protein adsorption, increasing ionic solubility and facilitating attachment points for osteoblasts. This is supported by Woesz et al. [13] who state that the nutrition of the cells within any structure must be ensured for viability, and that this is only possible via the flow of serum through both micro and macropores (pores $\geq$50 μm). Moreover, Yang et al. [14] reported the pore size requirements necessary for complete bone regeneration, Table 1.

In pursuit of a production method that will yield architectural characteristics similar to cancellous bone, a logical starting point would be to study techniques utilising the material itself. While organic free bovine bone is commercially available (Endobon®-Biomet, UK Ltd) the use of processed animal components, however, can elicit fears of disease transmission and immuno-rejection [15] Investigations attempting to replicate bovine cancellous bone, Tancred et al. [16], may raise similar concerns.

The obvious solution is to replicate human cancellous bone but this too has restrictions. Aside from the risk of bacterial contamination, viral transmission, and immunogenicity, there are logistical issues [17, 18]. According to Blom the supply of human bone simply cannot meet the demands of hip revision surgery let alone for all other operations requiring bone [19].

With concerns over contamination and disease transmission associated with processes using natural bone researchers have looked at other porous structures to mimic in their pursuit of developing the perfect bone substitute. In 1963 Brenzy and Green [20] patented a polymeric foam replication technique. The process, adopted by numerous authors [3, 20–26], involves the coating of open celled polymer foams with ceramic slurry followed by removal of the polymer through sintering. Despite subtle variations in processing techniques the scaffolds produced are highly porous ($\geq$70%) with characteristically round pores. The flexibility that comes from varying the characteristics of the polymer sponge allows for the production of scaffolds with controllable pore size [23]. Due to the isotropic nature of preform polymer sponges the pore size distribution in ceramic replicas is usually within tight bands of 200 μm at most, Table 2. According to Yang et al. [14] (Table 1) these distributions will be insufficient complete integration into the body.

For the scaffolds discussed in Table 2 interconnectivity between pores is inferred from high levels of porosity, fracture surface micrographs or pore window sizes [3, 20–26]. While claims of complete interconnectivity can be understood in some cases [24–26] (Fig. 1a–c), in others, without quantitative data, it would appear to be a massive assumption [3, 21, 22].

Recognising that nature's capabilities are significantly ahead of modern day technologies engineers continue to mimic, with varying degrees of success, the highly effective and energy efficient biological mechanisms found in

Table 1 Breakdown of scaffold pore size requirements for bone regeneration [14]

Scaffold pore size (μm)	Observations
5	Neovascularisation
15–40	Fibroblast ingrowth
40–100	Osteoid ingrowth
200–350	Significant bone ingrowth
>500	Rapid vascularisation

Table 2 Overview of structural characteristics and mechanical properties of scaffolds produced using the polymer foam replication technique

Material	Porosity (%)	Pore size distribution (μm)	Ref
45S5 Bioglass®	89–92	510–720	[21]
Glass Reinforced HA	85–97.5	420–560	[25]
HA	86	420–560	[21]
HA	69	490	[21]
HA	86	1130	[21]
HA	N/A	100–200	[22]
HA	70–77	200–400	[23]
HA	82–86	500–700	[24]
HA	87	150–200	[26]
HA	N/A	400–600	[3]

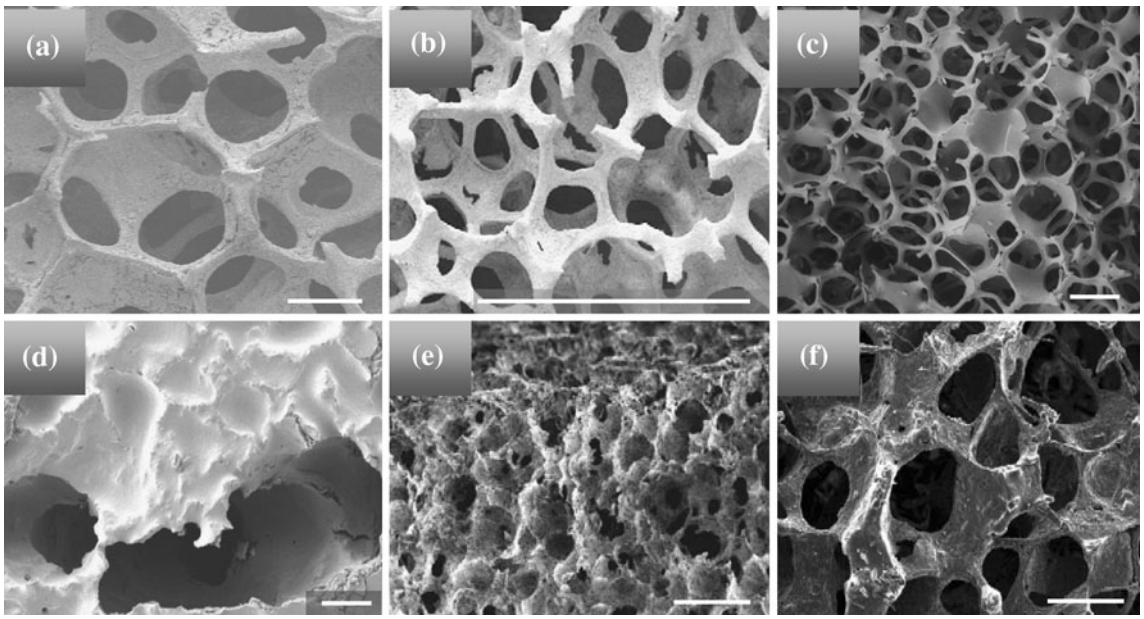

Fig. 1 Fracture surfaces of HA scaffolds produced via polymer sponge replication provided as evidence of pore interconnectivity by; **a** Kim et al. [24] **b** Kim et al. [26] **c** Callcut et al. [25] **d** Sopyan et al. [3] **e** Saiz et al. [22] and **f** Chen et al. [21] white scale bars all 500 μm

organisms around the world [17]. This field, known as biomimetics, bionics, or biogenesis, has reached astonishing levels that include simulation of the synaptic processes in the brain, imitating shark skin on the surface of ship propellers, duplicating the hearing of insects, the silk production of spiders and even traffic control of ants [11]. With regard to the development of bone substitutes, the past several years have seen various biomimetic approaches where attempts have been made to replicate the structure, chemical composition or growth of natural bone [27].

The merit in studying marine sponges as potential precursors in the production of tissue engineered (TE) bone scaffolds originates from their efficient interconnected porous architecture, which has evolved over millennia [28]. It has been reported that these sponges possess the ability to process a quantity of water corresponding to their own volume capacity every 5 s, equating to over one ton of water/day/kg of sponge [28]. Their natural functionality to facilitate the flow of fluid mimics that of an ideal bone scaffold material [28]. The challenge, therefore, was to source marine sponges with relevant pore architecture while developing and optimising the techniques required for their replication. Despite being posited by Rambo et al. [29], their use as preforms in the production of TE bone scaffolds, surprisingly, has up until now only been theorised (to the best of the authors' knowledge).

In pursuit of a production method that will yield architectural characteristics similar to trabecular bone, the following study, utilising a biomimetic approach, aims to demonstrate the reliable replication of the naturally interconnected porous structures of Dalmata Fina (*Spongia officinalis Linnaeus*), Fina Silk (*Spongia zimocca*) and Elephant Ear (*Spongia agaricina*) marine sponges and to show the repeatable production of complex 3D scaffolds with appropriate pore size distribution, and interconnection essential for successful bone ingrowth.

2 Materials and methods

2.1 Scaffold production

The marine sponges (Solihull, West Midlands, UK), harvested from controlled areas were inspected and certified for export by the Ministry of Agriculture and Fisheries (London, UK). The morphology of natural and replicated structures was determined using SEM (Jeol 6500 FEG-SEM, Tokyo, Japan).

After completely submerging 10 × 10 × 7 mm specimens of each sponge species in an optimised 80 wt% HA (Plasma Biotal Ltd. Batch P260/S/BM/192) solid loaded slip [30], each specimen was squeezed in a Collin W-100-T Two Roll Mill (LRS Planung and Technologie GMBH, Kaarst, Germany) with the rollers fixed at 3.5 mm apart. The specimens were then open air dried for 4 h, during which time they were turned every hour, followed by sintering in a box furnace (Elite Thermal Systems Ltd, Market Harborough, UK) at 1300°C. A ramp rate of 5°C min^{-1}, a cooling rate of 3°C min^{-1}, and a dwell time of 5 h were determined as the optimal sintering regime.

2.2 Micro CT analysis

Pore size distribution and degree of interconnectivity was determined using a MicroCT80 (Scanco Medical, Switzerland), operating at 70 kV with a voxel size of $50 \times 50 \times 50$ μm^3. Algorithms incorporated into the Scanco MicroCT80 software, used to quantify pore size distribution, were originally developed for determining trabecular strut thickness in bone. In order to facilitate the acquisition of pore size distribution data 2D images generated by the MicroCT80 were inverted and the pores treated as solid material. Once inverted, the algorithm worked by growing spheres from each pixel in the pore until it reached a boundary, in this case the nearest pixel representing the ceramic scaffold. From this, the cross sectional area of each pore was calculated. For each replicated preform investigated regions of $200 \times 200 \times 100$ voxels (equivalent to $10 \times 10 \times 5$ mm) were analysed. When analysing a porous structure made up of various grey scale voxels a threshold must be set distinguishing what is bone and what is empty space. After applying a threshold recommended by the software for analysis of bone the algorithm was applied.

The interconnectivity between the pores was quantified using 'Flood-fill' algorithms within the ScanCo software. These algorithms, also known as 'seed fill' algorithms, determine groups of neighbouring voxels (or nodes) of the same designation, that is 'pore' or 'ceramic', connected to each other within a given 3D array. The algorithm then ranks the groups of interconnected pores in terms of percentage from largest to smallest. In this case the 3D array is a 3D scan of a given scaffold. Taking a number of regions of interest and using a threshold recommended by the program for analysis of bone, the algorithm applied yielded the percentage interconnectivity for each scaffold analysed.

2.3 Mercury intrusion porosimetry

As the MicroCT equipment used a voxel size of $50 \times 50 \times 50$ μm^3, limited pore size distribution data could be gathered (that is pore $\leq$50 μm could not be quantified). Consequently, mercury intrusion porosimetry (MIP) was applied to gain a more in-depth understanding of the scaffolds' architecture. Residual moisture was removed by preheating the specimens at 300°C for 4 h, mercury (Hg) was incrementally forced through the porous constructs using a pressure of between 4 and 25 MPa. Upon each incremental rise in pressure an equilibrium time of 10 s was implemented prior to taking each reading of mean pore diameter, incremental and cumulative pore volume (ml/g) and pore area (m^2/g).

In instances where there are large internal pores accessible through narrow openings MIP has been reported to misrepresent the size of these pores as having the diameter of the narrow opening [31]. The error that arises due to the assumption that each pore is connected to the sample surface directly or via larger pores is referred to as the "*ink bottle*" effect [31, 32]. Despite this; determining pore window size, the total open porosity and verifying the presence of pores within the 1–50 μm range are essential to the overall characterisation of any scaffold.

3 Results

Figure 2 exhibits the three sponges; Elephant Ear (*Spongia agaricina)*, Fina Silk (*Spongia zimocca*) and Dalmata Fina (*Spongia officinalis Linnaeus*) in their natural and HA replicated condition along with SEM micrographs of the replicated TE bone scaffolds.

The intertwined fibrous struts of the natural Elephant Ear marine sponge (top row) which are on average 16 ± 8 μm thick and 20–30 μm apart form a mesh with regular macro pores of approximately 470 ± 120 μm. The macro pores are typically approximately 200–350 μm apart.

The Fina Silk (*Spongia zimocca*) (middle row) is typical of the overall size and morphology of the received batch. With a surface described by some authors as down (fine feather like) [33], the pores can be covered by the fibrous spongin network and difficult to see without cutting. The macro pores of the Fina Silk are sparse in comparison to those in the Elephant Ear (*Spongia agaricina)*. In this case the fibrous struts which are on average 15 ± 9 μm thick and 20–100 μm apart form a skeleton with irregular macro pores ranging from approximately 580–850 μm. The pores are approximately 600–1400 μm apart.

The overall morphology of Dalmata Fina (*Spongia officinalis* Linnaeus) (bottom row) is typically described as "*globular*" with typically large lobed-like growth characteristics [33]. The received consignment of Dalmata Fina (*Spongia officinalis* Linnaeus) fits this description. The architecture shown in Fig. 2 is composed of interwoven fibrous struts, approximately 5–40 μm apart, with an average thickness of 18.5 ± 10 μm which form a skeleton with macro pores ranging from approximately 580 μm–2 mm. The distance between pores varies between approximately 400–800 μm apart.

While the majority of the space between fibrous struts has been filled with the ceramic slip the macro pore patterns found on the surfaces of the natural preforms have been replicated in the ceramic constructs, as evident in Fig. 2.

While the results of mechanical integrity analysis are not shown (these will be reported in an upcoming paper) it should be noted that the replicas of each sponge exhibited a high degree of stability during handling and subsequent analysis.

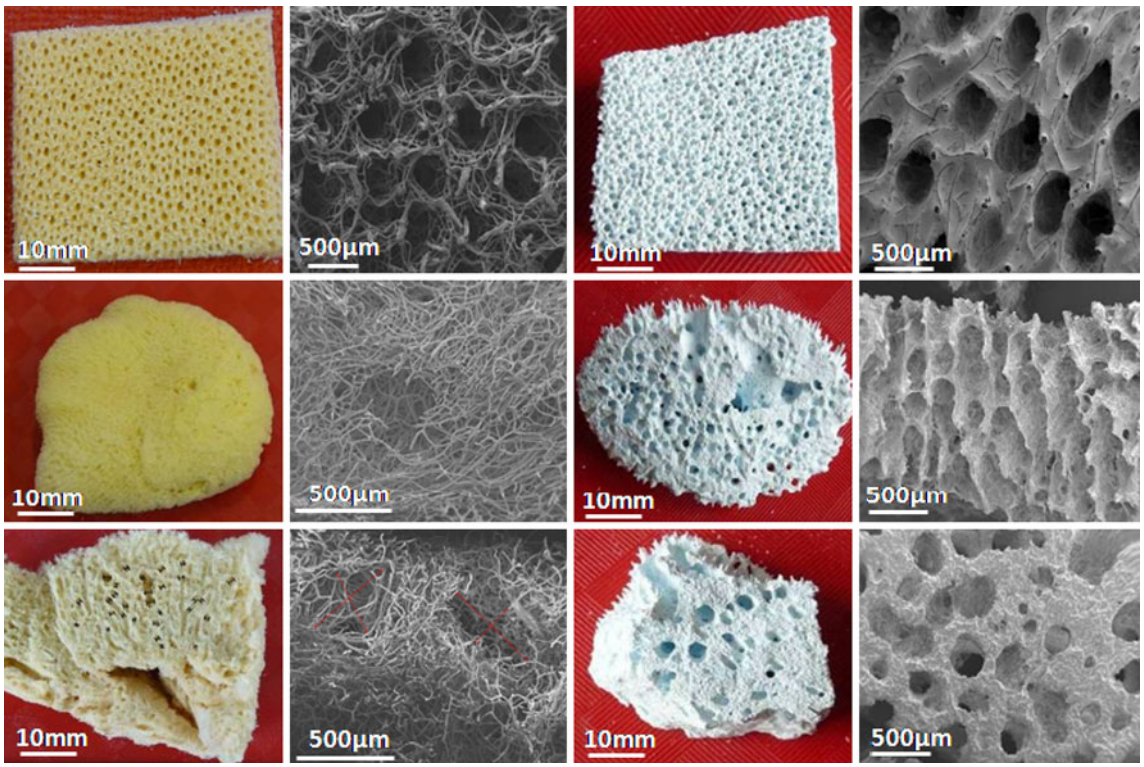

Fig. 2 (*Left* to *right*) natural bulk, natural SEM, HA TE replicated scaffold bulk and HA TE replicated scaffold SEM of (*Top*) elephant ear (*Spongia agaricina*) (*middle*) fina silk (*Spongia zimocca*) (*bottom*) dalmata fina (*Spongia officinalis* Linnaeus)

3.1 Micro-CT analysis

The Scanco MicroCT80 yielded the following pore size distribution data for the Elephant Ear, Fina Silk and Dalmata Fina HA based TE bone scaffolds (Fig. 3).

The 'floodfill' algorithm determined the level of interconnectivity between pores within each TE bone scaffold (Table 3). Average pore size, strut size and porosity were also quantified (Table 3).

As there is ambiguity in the literature relating to the range of pore sizes most ideal for bone ingrowth; the percentage of pores which fall into each has also been determined (Table 3).

Following from the MicroCT analysis, the TE bone scaffold replicated using the Elephant Ear sponge was deemed the optimal precursor material as it demonstrated architecture cited in literature as being ideal for successful integration into the body. It is also apparent from Table 3 that the Elephant Ear replicas are statistically more consistent than replicas of Dalmata Fina and Fina Silk. Therefore further analysis was conducted using only TE bone scaffold replicated using the Elephant Ear sponge.

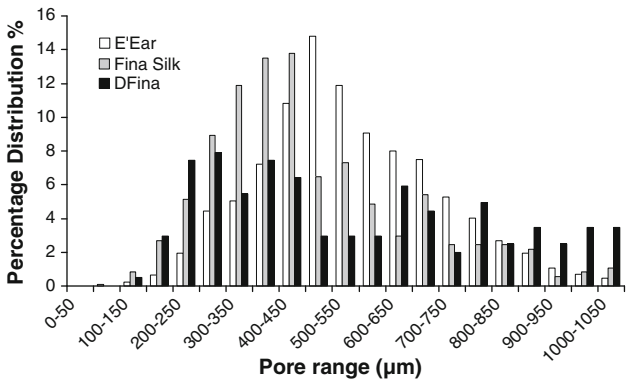

Fig. 3 Pores size distribution for TE bone scaffolds

3.2 Mercury intrusion porosimetry

TE bone scaffold replicated using the Elephant Ear sponge exhibited a bimodal pore distribution with peaks occurring at the micro (<20 µm) and macro (>50 µm) range. A lesser peak was also evident between 20 and 50 µm indicating that some pores within the scaffolds were at the meso-level (Fig. 4).

MIP analysis also yielded total surface area and total open porosity data. The two samples analysed, designated as sample 1 and sample 2 in Fig. 4, had a surface area of 35.67 and 40.77 m^2/g and open porosity values of 42.44 and 45.26%, respectively.

Table 3 Structural data and standard deviation determined by Scanco MicroCT80

	Elephant ear	Dalmata fina	Fina silk
Average interconnectivity value (%)	99.92 ± 0.1	90.701 ± 1.5	99.26 ± 0.4
Average pore size (μm)	349 ± 82	843 ± 316	444 ± 269
Average strut size (μm)	257 ± 95	1132 ± 448	508 ± 215
Average porosity (%)	55.6 ± 3.1	65.60 ± 5.4	62.90 ± 2.2
% Pores within 100–500 μm	83.1 ± 3.6	41.1 ± 7.2	63.2 ± 5.8
% Pores within 50–800 μm	97.7 ± 2	64.4 ± 3.8	88.7 ± 4.2

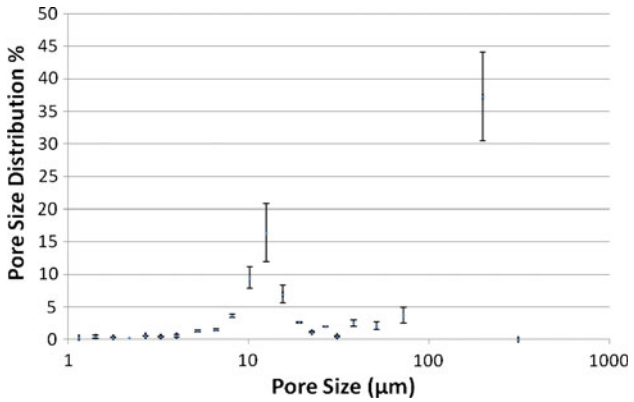

Fig. 4 Pore size distribution for elephant ear HA replicas determined using MIP

4 Discussion

In contrast with scaffolds developed utilising polymer foam replication techniques, which do not generally yield pores within the 0–200 μm range cited as necessary for complete integration with surrounding tissue [14], the use of natural marine sponge preforms addresses that need evident from the combined μ-CT, MIP and SEM results.

With regard to pore interconnectivity of the TE bone scaffolds produced, only the Dalmata Fina species had an interconnectivity of <99%. The TE scaffolds replicated using the Elephant Ear and Fina Silk species as precursors exhibited interconnectivity values of 99.92and 99.99%, respectively. While interconnectivity of the cited polymer replicated scaffolds was inferred from high levels of porosity and SEM images the 'floodfill' μ-CT algorithm used in this study provided quantitative evidence of the pore interconnectivity throughout each scaffold.

While using a 50 × 50 × 50 μm^3 voxel resolution may limit a full quantification of the entire spectrum of pore sizes, it is postulated that the scale of interconnectivity determined is more appropriate due to the general consensus that a minimum pore opening of ≥50 μm is required to facilitate cell and ion transport, and thus initiate osteogenesis [4, 12, 34–36].

In terms of the replication process each precursor marine sponges has been successfully infiltrated with the optimised 80 wt% solid loaded HA slip (reported previously by the author [30]). Despite a reduction in pore size between each natural sponge and its ceramic replica the investigation has provided clear evidence for the potential use of marine sponge precursors in TE bone substitute production.

5 Conclusion

The application of natural marine sponges in the development of ceramic based TE bone scaffolds, in particular Elephant Ear (*Spongia agaricina*), has been shown to have potential. It is proposed that the replication of Elephant Ear marine sponge allows for the reliable and repeatable production of HA scaffolds with the necessary characteristics to be used as a viable bone substitute material.

References

1. Jones JR, et al. Non-destructive quantitative 3D analysis for the optimisation of tissue scaffolds. Biomaterials. 2007;28(7):1404–13.
2. Karageorgiou V, Kaplan D. Porosity of 3D biomaterial scaffolds and osteogenesis. Biomaterials. 2005;26(27):5474–91.
3. Sopyan I, et al. Porous hydroxyapatite for artificial bone applications. Sci Technol Adv Mater. 2007;8(1–2):116–23.
4. von Doernberg M-C, et al. In vivo behavior of calcium phosphate scaffolds with four different pore sizes. Biomaterials. 2006; 27(30):5186–98.
5. Giannoudis PV, Dinopoulos H, Tsiridis E. Bone substitutes: an update. Injury. 2005;36(3, Supplement 1):20–7.
6. Engin NO, Tas AC. Manufacture of macroporous calcium hydroxyapatite bioceramics. J Eur Ceram Soc. 1999;19:2569–72.
7. Klawitter JJ, Hulbert SF. Application of porous ceramics for the attachment of load bearing internal orthopaedic applications. J Biomed Mater Res Symp. 1971;2(1):161–229.
8. Bohner M, Baumgart F. Theoretical model to determine the effects of geometrical factors on the resorption of calcium phosphate bone substitutes. Biomaterials. 2004;25(17):3569–82.
9. Bignon A, et al. Effect of micro- and macroporosity of bone substitutes on their mechanical properties and cellular response. Mater Med. 2003;14:1089–97.
10. Cyster LA, et al. The influence of dispersant concentration on the pore morphology of hydroxyapatite ceramics for bone tissue engineering. Biomaterials. 2005;26(7):697–702.
11. Mastrogiacomo M, et al. Role of scaffold internal structure on in vivo bone formation in macroporous calcium phosphate bioceramics. Biomaterials. 2006;27(17):3230–7.

12. Woodard JR, et al. The mechanical properties and osteoconductivity of hydroxyapatite bone scaffolds with multi-scale porosity. Biomaterials. 2007;28(1):45–54.
13. Woesz A, et al. Towards bone replacement materials from calcium phosphates via rapid prototyping and ceramic gelcasting. Mater Sci Eng C. 2005;25(2):181–6.
14. Yang SF. The design of scaffolds for use in tissue engineering. Part 1. Traditional factors. Tissue Eng. 2001;7(6):679–89.
15. Alisky JM. Xenografts are an achievable breakthrough. Med Hypotheses. 2004;63(1):92–7.
16. Tancred DC, McCormack BAO, Carr AJ. A synthetic bone implant macroscopically identical to cancellous bone. Biomaterials. 1998;19(24):2303–11.
17. Vaccaro A. The role of the osteoconductive scaffold in synthetic bone graft. Orthopaeadics. 2002;25(5):s571–8.
18. Hing KA, Wilson LF, Buckland T. Comparative performance of three ceramic bone graft substitutes. Spine J. 2007;7(4):475–90.
19. Blom A. (V) Which scaffold for which application? Curr Orthop. 2007;21(4):280–7.
20. Muhamad Nor MAA et al. Preparation and characterization of ceramic foam produced via polymeric foam replication method. J Mater Process Technol. 2008;(in press, corrected proof).
21. Chen QZ, Thompson ID, Boccaccini AR. 45S5 Bioglass derived glass ceramic scaffolds for bone tissue engineering. Biomaterials. 2006;27:2414–25.
22. Saiz E, et al. Preparation of porous hydroxyapatite scaffolds. Mater Sci Eng C. 2007;27(3):546–50.
23. Ramay HR, Zhang M. Preparation of porous hydroxyapatite scaffolds by combination of the gel-casting and polymer sponge methods. Biomaterials. 2003;24(19):3293–302.
24. Kim H-W, Knowles JC, Kim H-E. Hydroxyapatite porous scaffold engineered with biological polymer hybrid coating for antibiotic vancomycin release. J Mater Sci: Mater Med. 2005;16(3):189–95.
25. Callcut S, Knowles JC. Correlation between structure and compressive strength in a reticulated glass-reinforced hydroxyapatite foam. J Mater Sci: Mater Med. 2002;13(5):485–9.
26. Kim H-W, Knowles JC, Kim H-E. Hydroxyapatite/poly([var epsilon]-caprolactone) composite coatings on hydroxyapatite porous bone scaffold for drug delivery. Biomaterials. 2004;25(7–8):1279–87.
27. Zhang F, et al. Bioinspired structure of bioceramics for bone regeneration in load-bearing sites. Acta Biomater. 2007;3(6):896–904.
28. Müller WEG, et al. Traditional and modern biomedical prospecting: Part I—the history sustainable exploitation of biodiversity (sponges and invertebrates) in the Adriatic Sea in Rovinj (Croatia). Evid Based Complement Alternat Med (eCAM). 2004;1(1):71–82.
29. Rambo CR, et al. Biomimetic apatite coating on biomorphous alumina scaffolds. Mater Sci Eng C. 2006;26(1):92–9.
30. Cunningham E, et al. High-solid-content hydroxyapatite slurry for the production of bone substitute scaffolds. Proc Inst Mech Eng [H]. 2009;223(6):727–37.
31. Abell AB, Willis KL, Lange DA. Mercury intrusion porosimetry and image analysis of cement-based materials. J Colloid Interf Sci. 1999;211:39–44.
32. Moro F, Bohni H. Ink-bottle effect in mercury intrusion porosimetry of cement-based materials. J Colloid Interf Sci. 2001;246:135–49.
33. Pronzato R, Manconi R. Mediterranean commercial sponges: over 5000 years of natural history and cultural heritage. Mar Ecol. 2008;29:144–66.
34. Chang B-S, et al. Osteoconduction at porous hydroxyapatite with various pore configurations. Biomaterials. 2000;21(12):1291–8.
35. Gauthier O, et al. Macroporous biphasic calcium phosphate ceramics: influence of macropore diameter and macroporosity percentage on bone ingrowth. Biomaterials. 1998;19(1–3):133–9.
36. Le Huec JC, et al. Influence of porosity on the mechanical resistance of hydroxyapatite ceramics under compressive stress. Biomaterials. 1995;16(2):113–8.